Pakistan J. Zool., vol. 52(6), pp 2265-2273, 2020 DOI: https://dx.doi.org/10.17582/journal.pjz/20180719080742

The Use of Otolith Shape to Identify Stocks of Redlip Mullet, *Liza haematocheilus*

Tao He[1,2,3], Cheng-jing Chen[4], Jian-guang Qin[3], Yun Li[1,2], Rong-hua Wu[1,2] and Tian-xiang Gao[4,*]

[1]*College of Animal Science and Technology, Southwest University, Chongqing 400715, P.R. China*

[2]*Key Laboratory of Freshwater Fish Reproduction and Development (Ministry of Education), Key Laboratory of Aquatic Science of Chongqing 400715, P.R. China*

[3]*College of Science and Engineering, Flinders University, Adelaide 5001, Australia*

[4]*Fishery College, Zhejiang Ocean University, Zhoushan 316022, P.R. China*

ABSTRACT

The aim of this study was to compare sagittal morphometric features between *Liza haematocheilus* stocks in the China coasts at the Ying Kou, Dong Ying, Qing Dao, Wen Zhou and Guang Zhou regions and test a complementary method to quantify the variation of sagittal shapes to discriminate *L. haematocheilus* stocks. The sagitta variation of five *L. haematocheilus* stocks was examined using nine shape indices (Roundness, Circularity, Form-factor, Rectangularity, Ellipticity, Radius ratio, Feret ratio, Aspect ratio and Surface density). Multiple comparisons on shape indices showed that there was no significant difference among the Ying Kou and Dong Ying stocks, possibly due to their similar living habitat in the Bohai Sea. As the distribution zones of these five stocks are much overlapped, principal component analysis for otolith shape is not possible to distinguish *L. haematocheilus* stocks. Based on the Fourier coefficient, Fisher's discriminant analysis accurately classified 76.2% specimens into correct stocks whereas the discriminant function of shape indices only correctly identified 62.8% specimens into right stocks. As the sagittae in *L. haematocheilus* had an irregular round shape with many sharp notches, this study indicates that Fourier analysis is more suitable than shape indices to discriminate sagittae with irregular shapes. Our results demonstrate that as long as substantial intraspecific variations exist in sagittae shapes, geometric morphometrics for otolith shapes could be used as a complementary tool along with body morphology to distinguish *L. haematocheilus* stocks.

Article Information
Received 19 July 2018
Revised 03 September 2018
Accepted 19 September 2018
Available online 11 September 2020

Authors' Contribution
TH, CC and TG designed the study. TH, CC and RW conducted the field work and analyzed the sample. TH, JQ, YL and TG drafted the manuscript.

Key words
Redlip mullet, Otolith morphology, Shape indices, Fourier analysis, Discrimination function.

INTRODUCTION

Fish otoliths are composed of calcium carbonate crystals in a protein matrix. Calcium carbonate is usually deposited as aragonite on the saccule (sagittae) and utricle (lapillus) and as vaterite on the lagena (asteriscus) on different pieces of fish otolith (Oliveira *et al*., 1996; Falini *et al*., 2005). Among the components of fish otolith, the sagitta has the most remarkable feature as it shows a species-specific morphology but is less variable within a species (Campana, 2004). Morphological variation of sagittae can be influenced by age, genetic factors and environmental conditions (Vignon and Morat, 2010), and can also vary with growth rate, feeding history (Gagliano and McCormick, 2004) and habitat (Lombarte and Lleonart, 1993). Due to the influence of these complicated factors, the analysis of sagittal size and shape has become a useful tool for discriminating fish species and geographical stocks (Tuset *et al*., 2003).

Morphology of otolith shape has been widely used to distinguish phenotypic fish stocks as it is distinctly influenced by the environment and the habitats that fish live (Swain and Foote, 1999; Keating *et al*., 2014). Morphometry analysis can provide a quantitative description for shape and outline that can be statistically compared (Ibánez *et al*., 2017; Cheng *et al*., 2018). Many previous studies have used morphological characteristics to analyze and discriminate fish stocks or populations, especially using otolith morphology (Begg and Waldman, 1999; Adams *et al*., 2004).

The size-dependent variables of sagitta morphology include the anteroposterior length, maximal Feret's diameter, dorsoventral width, distance from the center to margins, area of 2-dimensional (2-D) sagittal projection and otolith perimeter (Ponton, 2006). The variation of these variables can be expressed as shape indices to differentiate geometric morphometrics of otoliths (Tuset *et al*., 2003). The image-dependent analysis of sagitta shapes such as Fourier analysis plays a significant role in morphometric studies, and represents an accurate method for characterizing otolith outlines and capturing contour variation (Cadrin and Friedland, 1999). In recent years,

* Corresponding author: gaotianxiang0611@163.com
0030-9923/2020/0006-2265 $ 9.00/0

Fourier analysis has been proved to be an efficient method for studying and describing contour shapes of an otolith (Cadrin and Friedland, 1999; Bani *et al*., 2013; Hüssy *et al*., 2016). This technique is useful for characterizing otolith morphometrics because: 1) the magnitude of contour variation associated with each harmonic measurement represents the contribution of a particular harmonic to the overall value of otolith morphometrics, and 2) the harmonics, when summed, can be used to recreate the otolith outline. The use of sagittal otolith morphology to identify different geographic stocks or populations has been reported in other fish species, such as silver hake *Merluccius bilinearis*, haddock *Melanogrammus aeglefinus*, king mackerel *Scomberomorus cavalla*, comber *Serranus cabrilla* , striped trumpeter *Latris lineate*, Atlantic molly *Poecilia mexicana*, roundnose grenadier *Coryphaenoides rupestris*, temperate seabass *Lateolabrax japonicas*; plainfin midshipman fish *Porichthys notatus* and white mullet *Mugil curema* (Bolles and Begg, 2000; Begg *et al*., 2001; DeVries *et al*., 2002; Tuset *et al*., 2003; Tracey *et al*., 2006; Schulz-Mirbach *et al*., 2010; Longmore *et al*., 2010; Fuji *et al*., 2014; Bose *et al*., 2017; Ibánez *et al*., 2017). Consequently, statistical analysis of otolith shape can be a powerful tool for fish stock management purposes (Hüssy *et al*., 2016), and has been already implemented in stock assessment (*e.g*., redlip mullet).

The redlip mullet *Liza haematocheilus* belongs to the family Mugilidae and is an important food fish distributed throughout China, Russia, Korea, and Europe (Li *et al*., 2006). This euryhaline estuarine-dependent fish, with a limited ability of migration, occurs in shallow coastal waters as well as estuarine freshwater regions (Gao *et al*., 2014). Because of good adaptability to an environment, fast growth rate, high productivity and favorable taste, *L. haematocheilus* has been an important species for marine aquaculture for decades (Meng *et al*., 2007). Han *et al*. (2013) compared the structure of population genetics among eight stocks of *L. haematocheilus* in north-western Pacific with amplified fragment length polymorphism markers, and found low genetic diversity between geographical populations. Gao *et al*. (2014) analyzed five populations from the coasts of China and Japan to investigate the genetic diversity and structure of redlip mullet based on sequence analysis of the mitochondrial DNA control region, examined its demographic history using neutrality tests and mismatch distribution analysis, and suggested this species was derived from a Pleistocene epoch population expansion. Recently, the analysis of cumulative otolith shape morphometric and microchemical of sagittal otoliths have been used to identify the presence of different mullet stocks in the southwestern region of the Atlantic Ocean (Fortunato *et al*., 2017).

However, to our best knowledge, there has been no study attempting to use morphometric indices analysis on *L. haematocheilus* otolith to differentiate fish stocks. As a complementary tool to differentiate redlip mullet stocks with body morphology, the morphometric analysis using multiple variables of the otolith could quantify the difference between otolith geometry. We hypothesize that the geometric morphometrics can detect the subtle difference between different stocks of *L. haematocheilus*, and offer a quantitative protocol to differentiate fish stocks in a fishing area. The aim of this study is to compare sagitta morphometric features between five locations of *L. haematocheilus* in China coast and test a complementary method to quantify the variation of sagitta shapes to discriminate *L. haematocheilus* stocks.

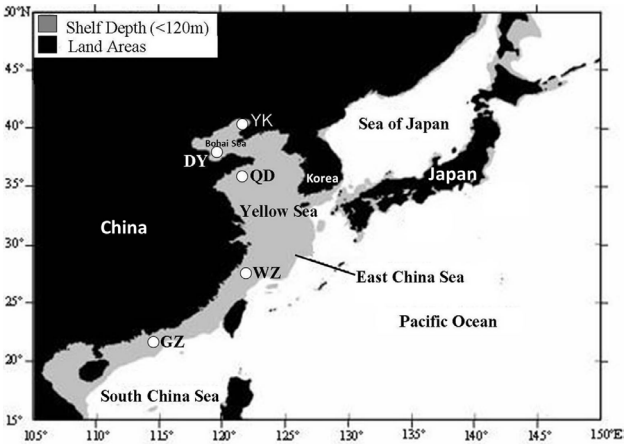

Fig. 1. Sampling locationsof five *L. haematocheilus:* Ying Kou (YK), Dong Ying (DY), Qing Dao (QD), Wen Zhou (WZ) and Guang Zhou (GZ).

Table I.- Sample information of five *L. haematocheilus* stocks.

Location	Date	Sample No.	Total length (mm)	Body length (mm)
Ying Kou	2010-01	23	257.2 ± 14.3	230.4 ± 12.8
Dong Ying	2009-09	55	133.9 ± 9.8	115.8 ± 8.7
Qing Dao	2009-11	31	242.3 ± 11.2	213.2 ± 10.9
Wen Zhou	2009-10	31	98.0 ± 7.1	82.5 ± 6.5
Guang Zhou	2011-02	21	332.9 ± 18.6	290.5 ± 17.5

MATERIALS AND METHODS

Sample collection

Fish were collected at Ying Kou (YK), Dong Ying (DY), Qing Dao (QD), Wen Zhou (WZ) and Guang Zhou (GZ), located along the south-east coast of China, from September 2009 to February 2011 (Fig. 1; Table I). The

sampling gear is a trawl. The sample from each location, was captured by three times, which could keep the diversity of the same stock, and the sample were preserved with the formaldehyde solution.

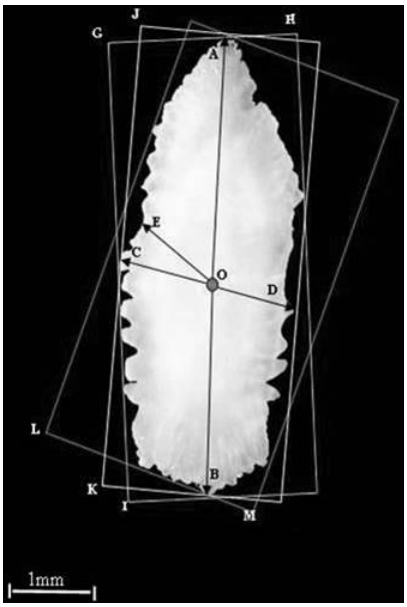

Fig. 2. Morphometric measurements of *L. haematocheilus* otolith O: core; OE: minimum radius; OA: maximum radius; LM: Feret width; JK: Feret length; GH: smallest Feret length; GI: longest Feret length. Bar = 1 mm.

Otoliths preparation

Both left and right sagittae were removed from each fish, and then cleaned with ultrasound (KQ3200) for 30 min to further remove tissue residuals and organics. Samples were then rinsed with Milli-Q water and left to dry overnight in a cupboard cabinet.

The left sagitta was examined and photographed using a Nikon SMZ8000 microscope equipped with a digital camera (Nikon SMZ1000). However, when the left sagitta was damaged, the right sagitta was used. If both otoliths were lost, the fish was discarded from the otolith shape analysis. Sagittae were positioned on a concave side before the image was taken. When the right otolith was used, the image was horizontally flipped using a standard image analysis technique to ensure that the rostrum was orientated to the right on the screen for each specimen.

Otolith shape analysis

The comparison of otolith shape was based on both the shape index analysis and Fourier analysis.

Shape index analysis

Using the image from each otolith, nine size parameters were calculated: Otolith weight (OW), area (A), perimeter (P), Feret length (FL), Feret width (FW), maximum radius (R_{max}), minimum radius (R_{min}), maximum Feret length (F_{max}) and minimum Feret length (Fig. 2; Table II). Feret length and Feret width are the length and width of a box, which encloses the trace of the otolith (Tuset *et al*., 2003). All measurements were taken using the Image-Pro Plus 6.0 program.

Nine shape indices were obtained by calculating the above nine parameters in various ways and the equations are presented in Table II. Roundness and circularity provide information on the similarity of various features to a perfect circle, taking a minimum value of 1 and 12.57, respectively. The form-factor is the mean value to estimate the irregularity of surface area, taking the value of 1.0 when it is a perfect circle and <1.0 when it is an irregular shape. Rectangularity describes the variations of length and width with respect to the area with the value of 1.0 being a perfect square. Ellipticity indicates if the changes in the axes are proportional (Russ, 1990).

Table II.- Multiple comparisons for sagittal shape indices of five *L. haematocheilus* stocks (Mean ± S.E.). For each morphometric index, the locations with the different letter were significantly different (P<0.05).

Size parameter	Shape index	Locations				
		Ying Kou	Dong Ying	Qing Dao	Wen Zhou	Guang Zhou
Area (A)	Roundness (V01)=4A/πFL^2	0.38±0.02^{ab}	0.38±0.03^{a}	0.36±0.02^{b}	0.42±0.02^{c}	0.38±0.02^{a}
Perimeter (P)	Form-factor (V02)=4πA/P2	0.48±0.04^{ab}	0.52±0.05^{ac}	0.46±0.04^{b}	0.51±0.06^{a}	0.47±0.04^{b}
Feret length (FL)	Circularity (V03)=P^2/A	26.17±2.03^{a}	24.48±2.67^{b}	27.57±2.45^{ac}	24.98±2.93^{ab}	26.94±2.37^{a}
Feret width (FW)	Rectangularity (V04)=A/(FL×FW)	0.71±0.02^{ac}	0.72±0.02^{a}	0.71±0.03^{a}	0.72±0.02^{ab}	0.71±0.03^{a}
Max radius (R_{max})	Ellipticity (V05)=(FL-FW)/(FL+FW)	0.41±0.02^{a}	0.41±0.03^{a}	0.43±0.03^{b}	0.38±0.02^{c}	0.41±0.02^{a}
Min radius (R_{min})	Radius ratio (V06)=R_{max}/R_{min}	3.06±0.23^{a}	2.96±0.24^{a}	3.40±0.34^{b}	2.58±0.16^{c}	3.07±0.18^{a}
Max Feret length (F_{max})	Feret ratio (V07)=F_{max}/F_{min}	2.44±0.14^{a}	2.45±0.17^{a}	2.58±0.17^{b}	2.25±0.09^{c}	2.40±0.13^{a}
Min Feret length (F_{min})	Aspect ratio (V08)=FL/FW	2.39±0.13^{a}	2.40±0.17^{a}	2.52±0.16^{b}	2.22±0.09^{c}	2.37±0.14^{a}
Otolith weight (OW)	Surface Density (V09) = OW/A	1.1×10^{-3}± 0.2×10^{-3}a	1.1×10^{-3}± 0.3×10^{-3}a	1.4×10^{-3}± 0.4×10^{-3}b	1.4×10^{-3}± 0.2×10^{-3}b	0.9×10^{-3}± 0.3×10^{-3}a

The radius ratio, Feret ratio and aspect ratio are the results of the division of the length by the width, and a larger value shows a more elongated shape (Ponton, 2006). Surface density indicates the thickness of otolith, and a higher value shows a thicker otolith.

Fourier analysis

The Fourier analysis decomposes the contour of an irregular 2-dimension image and forms a set of simpler components (harmonics) (Lestrel, 1997). Each successive harmonic can add more information on the property of shape morphometrics (Campana and Casselman, 1993). The Shape 1.3 software was used to extract the contours of the sagitta outline in preparation for Fourier analysis. The ChcViewer program generated a number of coordinates (x, y) best describing the outline shape of the sagitta. For each sagitta, 20 harmonics were generated using the CHC2NEF program. Each harmonic consisted of four coefficients resulting in 80 coefficients per otolith. The program standardizes the size and orientation, giving the first three coefficients with fixed values of A = 1, B = C = 0. Each individual was therefore represented by 77 unique coefficients (Longmore *et al*., 2010).

Principal component analysis

To reduce the dimensionality of the data, the principal component analysis was performed on both shape indices and Fourier coefficients by SPSS18.0. The significant principal components (PCs) were established according to the published methods (Duarte-Neto *et al*., 2008). The PC scores were used in the multivariate analysis between regions where fish were collected. Data were then tested for normality and homogeneity of variance using SPSS18.0. Any variables (shape indices/coefficients) that displayed a normal distribution and homogeneity of variance were tested for differences between sampling sites using univariate ANOVA (SPSS 18.0).

Discriminant function analysis

Fisher's discriminant function was used because it combines two or more measurements to improve the power to discriminate species (Goldstein and Dillon, 1978). Discriminant function analysis was carried out to determine the proportion of individuals that could be correctly assigned to their capture site based on sagittal shape variables (shape indices/coefficients). These variables were then tested for univariate correlation with otolith length and also correlation between variables to prevent any multicollinearity between variables as correlated variables can result in the use of redundant variables and a false outcome (Graham, 2003). Analysis of covariance was used to examine the influence of otolith length on each shape variable using SPSS 18.0.

RESULTS

Shape index analysis

No significant differences were found (MANOVA, $P = 0.05$) between the shape indices of right and left otoliths. Nine shape indices were tested for significant differences among five locations using one-way ANOVA ($P = 0.05$, Table II). There was no significant difference between YK and GZ stocks, but the shape indices of the YK stock were significantly different from the DY stock in the V03 index, QD stock in the V05-V09 indices, and WZ stock in the V01 and V05-V09 indices. Eight shape indices were significantly different between the DY and QD stocks, except the V04 index. The DY stock was significantly different from the WZ stock in the V01 and V05-V09 indices, and GZ stock in the V02 and V03 indices. Seven indices were significantly different between QD and WZ stocks, except the V03 and V04 indices. The QD stock was different from the GZ stock in the V01 and V05-V09 indices. Seven indices were significantly different between the WZ and GZ stocks, except the V03 and V04 indices.

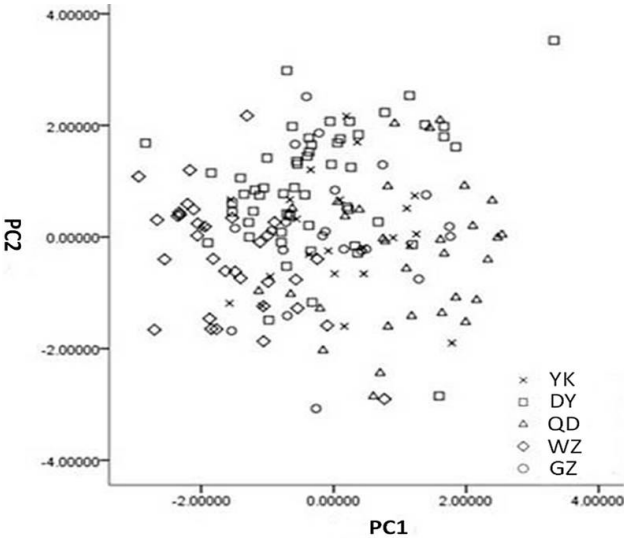

Fig. 3. Plots of the first two principal components (PC1 and PC2) of the shape indices in five *L. haematocheilus* stocks.

Principal component analysis showed that the first two PCs were relevant with eigenvalues of 4.83 and 2.20, respectively, according to the 'broken stick model' on sagittal contours (Jackson, 1993) and explained 78.06% of the overall variance (Supplementary Tables I, II). The first PC, accounting for 53.64% of the total variance, was mainly determined by four shape indices (V01, V05, V07 and V08). The second PC, accounting for 24.42% of the

variance, was mostly determined by the V02, V03, V04 and V09 indices. In the plot of the first two PCs (Fig. 3), the distribution zones of five stocks are heavily overlapped.

Table III.- Loadings of first two PCs for nine shape indices of *L. haematocheilus* otoliths.

PC	V01	V02	V03	V04	V05	V06	V07	V08	V09
PC1	-0.94	-0.63	0.66	-0.27	0.91	0.73	0.92	0.91	-0.10
PC2	-0.06	0.66	-0.65	0.65	0.39	-0.17	0.34	0.39	-0.68

Three shape indices (V02, V06 and V09) were screened by Fisher's discriminant analysis to establish the five discriminant functions for each stock:

YK: $Y_1 = 360.81X_1+74.01X_2+17472.07X_3–211.77$

DY: $Y_2 = 376.37X_1+73.22X_2+16776.95X_3–216.40$

QD: $Y_3 = 360.17X_1+79.95X_2+20633.71X_3–234.68$

WZ: $Y_4 = 360.93X_1+ 66.21X_2+19953.11X_3–193.00$

GZ: $Y_5 = 353.26X_1+73.64X_2+14612.71X_3–204.14$

Where, X_1 is V02, X_2 is V06 and X_3 is V09.

When the specimen was assigned, the three shape indices of each sagitta were substituted into the above five discriminant functions, and the corresponding maximum value (Y) indicated the attribution of each specimen. The results showed that the discriminant function analysis based on sagittal shape indices classified 62.8% of 161 individuals to the correct location (Table IV). Classification success was highest in the WZ stock with 90.9% of 31 individuals classified to their right sampling site. Classification success was 34.8% of 23 specimens in the YK stock, 51.8% of 55 individuals in the DY stock, 67.7% of 31 individuals in the QD stock, and 71.4% of 21 specimens in the GZ stock, respectively (Table IV).

Table IV.- Discriminant results of the otolith in five *L. haematocheilus* populations.

Stocks	Ying Kou	Dong Ying	Qing Dao	Wen Zhou	Guang Zhou	IA (%)
Ying Kou	8	5	3	4	3	34.8
Dong Ying	7	29	4	7	9	51.8
Qing Dao	4	2	21	0	4	67.7
Wen Zhou	1	1	0	30	1	90.9
Guang Zhou	2	2	1	1	15	71.4
TDA (%)						62.8

IA, identification accuracy; TDA, toal discriminant accuracy.

Fourier analysis

The first 20 harmonics explained at least 99.99% of the otolith variation. PCA was applied to selected Elliptical Fourier Descriptors matrix of otolith contours. Out of 77 Fourier coefficients (FCs) tested, only the first fifteen PCs were significant as determined by their eigenvalues exceeding the threshold eigenvalue (>1) generated by the broken-stick model and their cumulative contribution ratio accounted for 90.58% of the overall variance (Supplementary Table II). In the plot of the first two PCs (Fig. 4), the distribution zones of five stocks are totally overlapped.

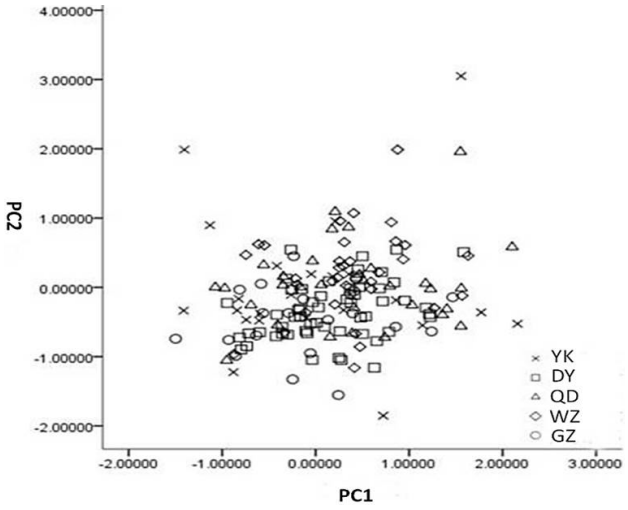

Fig. 4. Scatter plots of the first and second PC of *L. haematocheilus* sagittae based on Fourier analysis.

The shape variation (mean ± 2 SD; *i.e.* the square root of the eigenvalue of each component) was explained by the first 15 PCs (Supplementary Fig. S1). The principal characteristics mainly exhibited by the first four PCs (PC1 and PC2, the dorsal and ventral margins; PC3, the rostrum and posterior margin; PC4, the anterior-ventral margins). Therefore, the rostrum, and dorsal and ventral margins reflected the main variations between the five stocks.

In total, nine coefficients were chosen from 77 FCs by Fisher's discriminant analysis, and then were used to establish five discriminant functions:

YK: $Y_1 = 685.41X_1 – 62.46X_2 + 285.71X_3 – 131.70X_4 – 9.32X_5 + 11.13X_6 +240.29X_7 – 536.904X_8 + 118.76X_9 – 168.15$

DY: $Y_2 = 695.63X_1 – 144.03X_2 + 192.41X_3 – 110.84X_4 +204.98X_5 – 91.88X_6 +523.30X_7 – 459.28X_8 + 346.07X_9 – 162.10$

QD: $Y_3 = 650.85X_1 – 58.92X_2 + 332.78X_3 – 344.74X_4 + 37.49X_5 - 105.40X_6 +365.09X_7 – 314.40X_8 - 65.98X_9 – 152.51$

WZ: $Y_4 = 765.19X_1 – 179.42X_2 + 167.63X_3 – 170.10X_4 + 66.33X_5 – 376.36X_6 + 374.4X_7 – 517.36X_8 + 399.67X_9 – 190.48$

GZ: $Y_5 = 699.16X_1 – 50.10X_2 + 243.74X_3 – 21.96X_4$

$$- 34.51X_5 - 42.78X_6 + 124.70X_7 - 820.19X_8 + 641.30X_9 - 175.18$$

Where, X_1 is FC01, X_2 is FC06, X_3 is FC09, X_4 is FC17, X_5 is FC21, X_6 is FC25, X_7 is FC33, X_8 is FC43, and X_9 is FC67.

When the sample was assigned, the Fourier coefficients of each sagitta were substituted into the five discriminant functions, and the corresponding maximum value (Y) indicated the attribution of the samples. The discriminant function analysis classified 76.2% of overall 161 individuals to the initial locations based on the sagitta FCs (Table V). Classification success was highest in DY location with 85.7% of 55 individuals classified to their sampling site. Classification success was 56.5% of 23 samples in the YK location, 67.7% of 31 individuals in the QD location, 84.8% of 31 individuals in the WZ location, and 71.4% of 21 samples in the GZ location, respectively.

Table V.- Discriminant results of five *L. haematocheilus* stocks based on Fourier analysis.

Stocks	Ying Kou	Dong Ying	Qing Dao	Wen Zhou	Guang Zhou	IA (%)
Ying Kou	13	2	3	5	0	56.5
Dong Ying	4	48	2	2	0	85.7
Qing Dao	6	3	21	0	1	67.7
Wen Zhou	2	2	0	28	1	84.8
Guang Zhou	3	1	1	1	15	71.4
TDA (%)						76.2

IA, identification accuracy; TDA, toal discriminant accuracy.

DISCUSSION

Otolith morphology varies from a round shape in larval fish to an irregular shape in adult, and the shape indices represent the pattern of otolith growth in a bidimensional plane (Gauldie, 1988; Lagarde`re *et al*., 1995). Although the analysis of shape indices is complicated, it confirms that species identification can be made by the meristic characteristic of an otolith (Gaga, 1993; Tuset *et al*., 2003). In addition, the statistic analysis of otolith shapes is a more cost-effective and efficient method to differentiate fish stocks or populations than other methods such as the genetic marker discrimination technique, as recent divergence or secondary reproductive contact may result in no apparent difference in gene frequency between stocks (Begg and Waldman, 1999). In this study, the sagitta variation of five *L. haematocheilus* stocks was examined by using nine shape indices. Multiple comparisons of shape indices showed that there was no significant difference among the YK, DY and GZ locations. The possible explanation is that the YK and DY locations are distributed in a similar habitat in the Bohai Sea, resulting in the similar shape morphology of the otolith in these two stocks. Interestingly, although the GZ location is distributed in the South China Sea, which is far from the YK and DY locations, the shape indices of GZ location did not show significantly different from the YK and DY locations. Gao *et al*. (2014) tested the genetic diversity of five populations of *L. haematocheilus*, and the result showed that the nucleotide diversity of GZ and DY populations was similar, but was different from the QD and WZ stocks. So, YK, DY and GZ stocks could be classified as a group in this study.

The principal component analysis showed that the two PCs were mainly determined by eight shape indices out of the nine indices. As the distribution zones of the five stocks are overlapped on the plot, it is inferred that five stocks of *L. haematocheilus* are difficult to be discriminated by principal component analysis. Nevertheless, as Fisher's discriminant analysis can create a classified function to differentiate individuals within a group (Camacho, 1995), it differentiated the five stocks with the accuracy of 62.8% in this study. The identification accuracy on the WZ stock was highest, reaching 90.9%. Fortunato *et al*. (2017) used otolith shape indices to indentify the stocks of *Mugil liza* (Valenciennes 1836) in the Southwestern Atlantic Ocean and obtained a lower identification accuracy of 52.75%. In the present study, there was a high chance of fake discrimination among YK, DY and GZ locations because no significant difference can be found using multiple comparisons of shape indices among the three stocks. The discriminant function in this study was based on three shape indices (Form-Factor, Radius ratio and Surface Density), which may not be sensitive enough to discriminate the redlip mullet stocks. Bani *et al*. (2013) reported that the form factor, circularity, rectangularity, and aspect ratio indices are more efficient than other indices to differentiate south Caspian gobies, suggesting that the type of shape indices should be carefully chosen to establish a sensitive function to discriminate fish stocks using the analysis of otolith shape indices.

Fourier coefficients of otoliths have been used to detect the differences among herring (*Clupea harengus*) stocks (Bird *et al*., 1986). The use of elliptic Fourier descriptors can highly discriminate different Atlantic salmon (*Salmo salar*) stocks (Pontual and Prouzet, 1987). In recent years, Fourier analysis has been proved to be an efficient method for studying and describing contour shapes of an otolith (Cadrin and Friedland, 1999; Bani *et al*., 2013; Hüssy *et al*., 2016). In the present study, as the first two Fourier coefficients accounted for 36.93% of the overall variance in the principal component analysis, the distribution zones of five stocks are overlapped in the plot, which is similar to the result from shape indices analysis.

Consequently, principal component analysis for otolith shape could not efficiently distinguish *L. haematocheilus* stocks in this study.

Fisher's discriminant analysis classified 76.2% of individuals into correct stocks based on Fourier coefficients, which is a better method than the discriminant function using shape indices with only 62.8% accuracy for stock identification. The one possible reason is the Fourier descriptors are a description of the outline and the morphometric indices are only some proxies of the outline. There is not the same level of precision. Another possible reason is that, the shape of *L. haematocheilus* sagittae is round with many sharp notches on the edge, resulting in irregular otolith shape. The shape index has higher classification accuracy on sagittae with a regular shape than with an irregular shape. Fourier analysis, on the other hand, can efficiently capture outline information for an otolith with complex and irregular shapes (Lestrel, 1997). Therefore, the Fourier analysis is more suitable to detect the variation of otoliths with irregular shapes like *L. haematocheilus* stocks.

CONCLUSION

Substantial intraspecific variations exist in sagitta shapes among *L. haematocheilus* stocks. Fisher's discriminant analysis is able to distinguish *L. haematocheilus* stocks based on the morphology of sagitta shapes. Based on the Fourier coefficient, Fisher's discriminant analysis accurately classified 76.2% specimens into correct stocks whereas the discriminant function of shape indices only correctly identified 62.8% specimens into right stocks. As the sagittae in *L. haematocheilus* had an irregular round shape with many sharp notches, this study indicates that Fourier analysis is more suitable than shape indices to discriminate sagittae with irregular shapes. In conclusion, morphometric analysis of otolith shapes could be used as a complementary tool along with body morphology to distinguish fish stocks.

ACKNOWLEDGEMENTS

This research is funded by National Natural Science Foundation of China (No. 41506158, 41776171), International Science and Technology Cooperation Program of China (No. 2015DFR30450), Public Science and Technology Research Funds Projects of Ocean (No. 201505025),Chongqing Research Program of Basic Research and Frontier Technology (No. CSTC2016JCYJA0327), Genetic Resources Conservation Grant (Fisheries) from Ministry of Agriculture of the P. R. China (No. 171721301354052181) and Ecological Fishery Industrial Technology System Project from Chongqing Municipal Agriculture Commission (Grant to YL). Fundamental Research Funds for the Central Universities (Grant Number: XDJK2016C016). Tao He is grateful for the support of the China Scholarship Council with visiting scholar programs to Flinders University. All procedures performed were complied with the ethical standards and guidelines of Zhejiang Ocean University of China.

Supplementary material

There is supplementary material associated with this article. Access the material online at: https://dx.doi.org/10.17582/journal.pjz/20180719080742

Statement of conflict of interest

The authors have declared no conflict of interest.

REFERENCES

Adams, D.C., Rohlf, F.J. and Slice, D.E., 2004. Geometric morphometrics: Ten years of progress following the 'revolution'. *Italian J. Zool.,* **71**: 5-16. https://doi.org/10.1080/11250000409356545

Bani, A., Poursaeid, S. and Tuset, V.M., 2013. Comparative morphology of the sagittal otolith in three species of south Caspian gobies. *J. Fish Biol.,* **82**: 1321-1332. https://doi.org/10.1111/jfb.12073

Begg, G.A. and Waldman, J.R., 1999. An holistic approach to fish stock identification. *Fish. Res.,* **43**: 35-44. https://doi.org/10.1016/S0165-7836(99)00065-X

Begg, G.A., Overholtz, W.J. and Munroe, N.J., 2001. The use of internal otolith morphometrics for identification of haddock (*Melanogrammus aeglefinus*) stocks on Georges Bank. *Fish. Bull.,* **99**: 1-14.

Bird, J.L., Eppler, D.T. and Checkley, D.M., 1986. Comparisons of herring otoliths using Fourier series shape analysis. *Canadian J. Fish. aquat. Sci.,* **43**: 1228-1234. https://doi.org/10.1139/f86-152

Bolles, K.L. and Begg, G.A., 2000. Distinction between silver hake (*Merluccius bilinearis*) stocks in U.S. waters of the northwest Atlantic based on whole otolith morphometrics. *Fish. Bull.,* **98**: 451-462.

Bose, A.P., Adragna, J.B. and Balshine, S., 2017. Otolith morphology varies between populations, sexes and male alternative reproductive tactics in a vocal toadfish *Porichthys notatus*. *J. Fish Biol.,* **90**: 311-325. https://doi.org/10.1111/jfb.13187

Cadrin, S.X. and Friedland, K.D., 1999. The utility of image processing techniques for morphometric analysis and stock identification. *Fish. Res.,*

43: 129-139. https://doi.org/10.1016/S0165-7836(99)00070-3

Camacho, J., 1995. *Ana´ lisis multivariado con SPSS/PC+*. EUB, Barcelona. 348.

Campana, S.E., 2004. *Photographic atlas of fish otoliths of the Northwest Atlantic ocean*. Canadian Special Publication of Fisheries and Aquatic Sciences No. 133, NRC Research Press.

Campana, S.E. and Casselman, J.M., 1993. Stock discrimination using otolith shape analysis. *Canadian J. Fish. aquat. Sci.,* **50**: 1062-1083. https://doi.org/10.1139/f93-123

Cheng, D., Hassan, M.M., Ma, Z., Yang, Q. and Qin, J., 2018. Skeletal ontogeny and anomalies in larval and juvenile crimson snapper, *Lutjanus erythropterus* Bloch, 1790. *Pakistan. J. Zool.,* **50**: 799-807

DeVries, D.A., Grimes, C.B. and Prager, M.H., 2002. Using otolith shape analysis to distinguish eastern Gulf of Mexico and Atlantic Ocean stocks of king mackerel. *Fish. Res.,* **57**: 51-62. https://doi.org/10.1016/S0165-7836(01)00332-0

Falini, G., Fermani, S., Vanzo, S., Miletic, M. and Zaffino, G., 2005. Influence on the formation of aragonite or vaterite by otolith macromolecules. *Eur. J. Inorg. Chem.,* **2005**: 162-167. https://doi.org/10.1002/ejic.200400419

Duarte-Neto, P., Lessa. Rn., Stosic, B. and Morize, E., 2008. The use of sagittal otoliths in discriminating stocks of common dolphinfish (*Coryphaena hippurus*) off northeastern Brazil using multishape descriptors. *ICES. J. Mar. Sci.,* **65**: 1144-1152.

Fortunato, R.C., González-Castro, M., Galán, A.R., Alonso, I.G., Kunert, C., Durà, V.B. and Volpedo, A., 2017. Identification of potential fish stocks and lifetime movement patterns of *Mugil liza* Valenciennes 1836 in the Southwestern Atlantic Ocean. *Fish. Res.,* **193**: 164-172. https://doi.org/10.1016/j.fishres.2017.04.005

Fuji, T., Kasai, A., Ueno, M. and Yamashita, Y., 2014. Growth and migration patterns of juvenile temperate seabass *Lateolabrax japonicus* in the Yura River estuary, Japan-combination of stable isotope ratio and otolith microstructure analyses. *Environ. Biol. Fishes,* **97**: 1221-1232. https://doi.org/10.1007/s10641-013-0209-4

Gaga, F.J., 1993. Morphology of the saccular otoliths of six species of lanternfishes of the Genus Symbolophorus (Pisces: Myctophidae). *B. Mar. Sci.,* **52**: 949-960.

Gagliano, M. and McCormick, M.I., 2004. Feeding history influences otolith shape in tropical fish. *Mar. Ecol. Progr. Ser.,* **278**: 291-296. https://doi.org/10.3354/meps278291

Gao, T., Li, Y., Chen, C., Song, N. and Yan, B., 2014. Genetic diversity and population structure in the mtDNA control region of *Liza haematocheilus* (Temminck & Schlegel, 1845). *J. appl. Ichthyol.,* **30**: 941-947. https://doi.org/10.1111/jai.12409

Gauldie, R.W., 1988. Function, form and time-keeping properties of fish otoliths. *Comp. Biochem. Physiol.,* **91**: 395-402. https://doi.org/10.1016/0300-9629(88)90436-7

Graham, M.H., 2003. Confronting multicollinearity in ecological multiple regression. *Ecology,* **84**: 2809-2815.

Goldstein, M. and Dillon, W.R., 1978. *Discrete discriminant analysis.* Wiley, New York. pp. 186.

Han, Z.Q., Han, G., Gao, T.X., Wang, Z.Y. and Shui, B.N., 2013. Genetic population structure of *Liza haematocheilus* in north-western Pacific detected by amplified fragment length polymorphism markers. *J. mar. Biol. Assoc. U.K.,* **93**: 373-379. https://doi.org/10.1017/S0025315412000872

Ibáñez, A.L., Hernández-Fraga, K. and Alvarez-Hernández, S., 2017. Discrimination analysis of phenotypic stocks comparing fish otolith and scale shapes. *Fish. Res.*, **185**: 6-13. https://doi.org/10.1016/j.fishres.2016.09.025

Hüssy, K., Mosegaard, H., Albertsen, C.M., Nielsen, E.E., Hemmer-Hansen, J. and Eero, M., 2016. Evaluation of otolith shape as a tool for stock discrimination in marine fishes using Baltic Sea cod as a case study. *Fish. Res.*, **174**: 210-218. https://doi.org/10.1016/j.fishres.2015.10.010

Keating, J.P., Brophy, D., Officer, R.A. and Mullins, E., 2014. Otolith shape analysis of blue whiting suggests a complex stock structure at their spawning grounds in the Northeast Atlantic. *Fish. Res.*, **157**: 1-6. https://doi.org/10.1016/j.fishres.2014.03.009

Jackson, D.A., 1993. Stopping rules in principal components analysis: A comparison of heuristical and statistical approaches. *Ecology*, **74**: 2204-2214. https://doi.org/10.2307/1939574

Lagarde`re, F., Chaumillon, G., Amara, R., Heineman, G. and Lago, J.M., 1995. Examination of otolith morphology and microstructure using laser scanning microscopy. In: *Recent developments in fish Otolith research* (eds. D.H. Secor, J.M. Dean and S.E. Campana). University of South Carolina Press, South Carolina, pp. 7-26.

Lestrel, P.E., 1997. Introduction and overview of Fourier descriptors. In: *Fourier descriptors and their applications in biology* (ed. P.E. Lestrel). Cambridge University Press, Cambridge, UK, pp. 22-44.

https://doi.org/10.1017/CBO9780511529870.003

Li, A., Hu, J., Zhang, Z. and Yang, M., 2006. Quantitative real-time RT-PCR for determination of vitellogenin mRNA in so-iuy mullet (*Mugil soiuy*). *Analyt. Bioanalyt. Chem.*, **386**: 1995-2001. https://doi.org/10.1007/s00216-006-0846-y

Lombarte, A. and Lleonart, J., 1993. Otolith size changes related with body growth, habitat depth and temperature. *Environ. Biol. Fishes*, **37**: 297-306. https://doi.org/10.1007/BF00004637

Longmore, C., Fogarty, K., Neat, F., Brophy, D., Trueman, C. and Milton, A., 2010. A comparison of otolith microchemistry and otolith shape analysis for the study of spatial variation in a deep-sea teleost, *Coryphaenoides rupestris*. *Environ. Biol. Fishes*, **89**: 591-605. https://doi.org/10.1007/s10641-010-9674-1

Meng, W., Gao, T. and Zheng, B., 2007. Genetic analysis of four populations of redlip mullet (*Chelon haematocheilus*) collected in China Seas. *J. Ocean Univ. China*, **6**: 72-75. https://doi.org/10.1007/s11802-006-0072-z

Oliveira, A.M., Farina, M., Ludka, I.P. and Kachar, B., 1996. Vaterite, calcite, and aragonite in the otoliths of three species of piranha. *Naturwissenschaften*, **83**: 133-135. https://doi.org/10.1007/BF01142180

Ponton, D., 2006. Is geometric morphometrics efficient for comparing otolith shape of different fish species? *J. Morphol.*, **267**: 750-757. https://doi.org/10.1002/jmor.10439

Pontual, H. and Prouzet, P., 1987. Atlantic salmon, *Salmo salar* L., stock discrimination by scale-shape analysis. *Aquacul. Fish. Manage.*, **18**: 277-289. https://doi.org/10.1111/j.1365-2109.1987.tb00147.x

Russ, J.C., 1990. *Computer-assisted microscopy: The measurement and analysis of images.* Plenum Press, New York.

Schulz-Mirbach, T., Ladich, F., Riesch, R. and Plath, M., 2010. Otolith morphology and hearing abilities in cave- and surface-dwelling ecotypes of the Atlantic molly, *Poecilia mexicana* (Teleostei: Poeciliidae). *Hear. Res.*, **267**: 137-148. https://doi.org/10.1016/j.heares.2010.04.001

Swain, D.P. and Foote, C.J., 1999. Stocks and chameleons: The use of phenotypic variation in stocks identification. *Fish. Res.*, **43**: 113-128. https://doi.org/10.1016/S0165-7836(99)00069-7

Tracey, S.R., Lyle, J.M. and Duhamel, G., 2006. Application of elliptical Fourier analysis of otolith form as a tool for stock identification. *Fish. Res.*, **77**: 138-147. https://doi.org/10.1016/j.fishres.2005.10.013

Tuset, V.M., Lozano, I.J., Gonzalez, J.A., Pertusa, J.F. and Garcia-Diaz, M.M., 2003. Shape indices to identify regional differences in otolith morphology of comber, *Serranus cabrilla* (L., 1758). *J. appl. Ichthyol.*, **19**: 88-93. https://doi.org/10.1046/j.1439-0426.2003.00344.x

Vignon, M. and Morat, F., 2010. Environmental and genetic determinant of otolith shape revealed by a non-indigenous tropical fish. *Mar. Ecol. Progr. Ser.*, **411**: 231-241. https://doi.org/10.3354/meps08651